PAPER

A low-complexity photoplethysmographic systolic peak detector for compressed sensed data

IOP Publishing Physiol. Meas. 40 (2019) 065007 (15pp) https://doi.org/10.1088/1361-6579/ab254b

Physiological Measurement

IPEM Institute of Physics and Engineering in Medicine

PAPER

A low-complexity photoplethysmographic systolic peak detector for compressed sensed data

RECEIVED
4 March 2019

REVISED
23 May 2019

ACCEPTED FOR PUBLICATION
29 May 2019

PUBLISHED
2 July 2019

Giulia Da Poian[1], Nunzio A Letizia[2], Roberto Rinaldo[2] and Gari D Clifford[1,3]

[1] Department of Biomedical Informatics, Emory University, Atlanta, GA, United States of America
[2] Dipartimento Politecnico di Ingegneria e Architettura, University of Udine, Udine, Italy
[3] Department of Biomedical Engineering, Georgia Institute of Technology, Atlanta, GA, United States of America

E-mail: giulia@dbmi.emory.edu

Keywords: compressive sensing, PPG, peak detection, compressive signal processing, compressive peak detection

Abstract

Objective: Recent advances in wearable technologies and signal processing have made it possible to perform health monitoring during everyday life activities. Despite the fact that new technologies allow the storage of large volumes of data on small devices, limitations remain when data have to be transmitted or processed with devices with both energy and computational constraints. *Approach*: This work focuses on the implementation and validation of a photoplethysmogram (PPG) low-complexity analysis method for sensors that acquire a compressed PPG signal through compressive sensing (CS) and allows for the accurate detection of the PPG systolic peak in the compressed domain. Three public datasets were used consisting of a total of about 52 h of PPG signals from 600 patients with normal and abnormal rhythms. Peaks were manually annotated by experts or derived from the annotated synchronized ECG. *Main results*: The proposed method achieved a pooled average F1 measure on the three datasets of 91% ± 8% for a 5% compression ratio (CR), 89% ± 10% for CR = 70% and 82% ± 12% for CR of 90%. The pooled average F1 measure on the original uncompressed data using an offline open source peak detector is F1 = 91% ± 11%. The proposed method is up to ∼100 times faster with respect to methods using decompression followed by peak detection. *Significance*: Results demonstrate that it is possible to achieve detection performance, in terms of the F1 measure, comparable with those obtained on the original uncompressed and filtered signal, making the proposed approach appropriate for real-time wearable systems with energy and computation constraints.

1. Introduction

In the last decade there has been an increasing interest on the development of new wearable technologies for health monitoring (Pantelopoulos and Bourbakis 2010, Seneviratne *et al* 2017). As a consequence of aging populations, dysfunctional lifestyles, and the rising concern of patients toward their health, many studies have been focused on new solutions to provide real-time and continuous monitoring of physiological parameters. However, to make it possible for wearable devices to cross the boundary between consumer electronics devices, with a simple fitness monitoring purpose, to regulated medical devices, new algorithms and methods are needed. Indeed, it is necessary to ensure a certain quality of the acquired signal as well as to preserve the diagnostic information while processing the signals (Shcherbina *et al* 2017).

While devices are becoming smaller and sensors integrated in everyday objects (e.g. watches, clothing ...), there are still some technology limitations to make it possible to continuously monitor the health status in real-time. The huge storage capacity available even on small devices leverages somehow the problem when non immediate processing of the signal is required. Also, cloud storage and cloud computing seems to be very promising to this end, but they both require to transfer the data from the wearable device to the cloud platform, usually by Bluetooth/wireless connection.

When continuous transmission of the data is required, for example between the sensors to a smart-phone via Bluetooth, or to a remote cloud platform over Wi-Fi, energy limitations start to become predominant. To man-

age energy-related issues, one of the most promising and extensively investigated solutions proposed over the last years is compressive sensing (CS) (Candès and Wakin 2008).

As shown by several works (Chen *et al* 2012, Dixon *et al* 2012, Liu *et al* 2014, Craven *et al* 2015), CS allows to extend the battery life of a low-power device, by acquiring a compressed version of the signal at a lower rate with respect to the one required by Nyquist, and avoiding the compression stage. It should be noted that CS can be also implemented as a low complexity (and low consumption) digital compression scheme (Da Poian *et al* 2016, Pareschi *et al* 2017).

In this study we consider the scenario of a photoplethysmographic (PPG) sensor designed to directly acquire a compressed sensed version of the original PPG signal (Rajesh *et al* 2016, Natarajan *et al* 2017, Pamula *et al* 2018). The one proposed by Rajesh *et al* (2016) is also able to perform a direct estimation of the average heart-rate (HR) over a 4 s window without signal decompression, by using the power spectral density obtained from the Lomb–Scargle periodogram.

Similarly, the recently proposed TROIKA (Zhang *et al* 2015) and JOSS (Zhang 2015) methods are able to perform HR estimation from down-sampled PPG signals. Both methods apply signal processing to remove motion artefacts from the PPG spectra prior to HR estimation by choosing the highest spectral peak in the PPG spectrum. The TROIKA framework consists of signal decomposition (which aims to partially remove the motion artefact components), sparsity-based high-resolution spectrum estimation, and spectral peak tracking and verification. The JOSS method jointly estimates spectra of PPG signals and simultaneous acceleration signals, utilizing the multiple measurement vector model in sparse signal recovery, to remove motion artefact from the PPG spectra. The processing/analysis capability of these methods is limited to HR estimation and do not provide inter-beat-interval (IBI) estimation.

The aim of this research goes beyond HR estimation by developing and validating a compressed PPG systolic peak detection system, inspired by the method proposed for the ECG signal in Da Poian *et al* (2017). The proposed framework, hereinafter called *CSMFppg*, works on the compressed signal without need of signal reconstruction (i.e. decompression). In particular, it is able to detect the PPG systolic peaks useful to perform pulse rate variability (PRV) analyses as well as atrial fibrillation (AF) detection, and HR as well. As reported in Schäfer and Vagedes (2013), PRV is typically sufficiently accurate, although coupling effects between respiration and the cardiovascular system leads to an overestimation of the short-term variability.

In this work we present an efficient processing algorithm for compressed detection of PPG systolic peaks with the future aim of developing an event driven wearable PPG monitoring device, which after detecting an abnormal event—such as AF—on the compressed signal, can send an alert as well as the compressed signal to a remote user, e.g. a physician. Furthermore, the compressed signal can be always recovered at the receiver by solving an optimization problem (see section 1.1) combined with a sparsyfing basis such as the one we propose in this paper (see section 2.3), allowing for further analysis and expert evaluation.

The main contributions of this paper are as follows:

- low complexity digital processing of PPG signals—the systolic peaks are estimated directly from sub-Nyquist samples;
- novel dictionary for PPG spare approximation that exploits the structure of the signal and that improves the reconstruction performance;
- validation of proposed methods on a broad set of PPGs different for patient age, recording device (wrist and fingertip), health status and activity (rest and physical exercise).

1.1. Compressive sensing of PPG signal

This section is intended to introduce the notation used in the rest of this work. For an extensive review of the compressive sensing technique please refer to Candès and Wakin (2008). Let us consider a PPG signal $x(t)$, which is going to be acquired and simultaneously compressed. By using compressive sensing it is possible to merge the acquisition and compression stage in order to directly acquire a signal $\mathbf{y} \in \mathbb{R}^M$, which is a compressed digitized version of the original signal samples $\mathbf{x} \in \mathbb{R}^N$, relative to a fixed window of length N. This operation can be mathematically expressed as

$$\mathbf{y} = \Phi\mathbf{x} + \mathbf{n}, \tag{1}$$

where $\Phi \in \mathbb{R}^{M\times N}$, with $M < N$, is the so called *sensing matrix*, which must satisfy the restricted isometry property (RIP) (Baraniuk *et al* 2008) in order to preserve information during compression. The additional term $\mathbf{n}$ represents the measurement and process noise.

Signal reconstruction, sometimes referred to as recovery or decompression, can be performed by optimization methods exploiting the sparsity of the acquired signal. Given a basis $\Psi \in \mathbb{R}^{N\times N}$ or an overcomplete dictionary $\mathbf{D} \in \mathbb{R}^{N\times P}$, with $P > N$, a signal is said to be k-sparse if its signal expansion $\alpha, \alpha \in \mathbb{R}^P$ such that $\mathbf{x} = \mathbf{D}\alpha$

has only k non zero elements, with $k \ll N$. Thus, given a sparsifying dictionary (or basis), one can recover the signal $\mathbf{x}$ from the compressed measurements $\mathbf{y}$, by solving the following optimization problem:

$$\min_{\alpha} ||\alpha||_0 \text{ s.t. } ||\mathbf{y} - \Phi\mathbf{D}\alpha||_2^2 \leqslant \epsilon, \tag{2}$$

and obtain $\mathbf{x}$ as $\mathbf{x} = \mathbf{D}\alpha$. This NP-hard problem can be solved by several methods proposed in literature such as basis pursuit denoising (BPDN) (Chen *et al* 2001), orthogonal matching pursuit (OMP) (Tropp and Gilbert 2007), Smooth-*l*0 (SL0) (Mohimani *et al* 2009).

2. CSMFppg algorithm description

Inspired by the compressed sensed matching filtering (CSMF) ECG peak detector (Da Poian *et al* 2017), implemented for beat detection on compressed sensed ECG signals, in this work we propose a compressed systolic peak detector for the PPG signal. Note that the proposed signal modeling and processing procedures differ from the ones presented in Da Poian *et al* (2017), which are tailored to ECG, in particular for template generation and compressive sensing dictionary construction.

2.1. Template generation

The PPG systolic peak detector used in this work is based on the estimated correlation of the compressed input signal $\mathbf{y}$ with a known template γ, which is projected into the compressed domain as well.

The first and fundamental step is the construction of the template γ on the uncompressed or reconstructed signal. To this end we assume to have access to a limited portion of good quality uncompressed signal $\mathbf{x_{int}}$ of length T_{int}. In a real-world application one can provide for a preliminary phase, in which the subject is asked to record an initialization signal for T_{int} seconds, without movements to guarantee a good signal quality. When only the compressed sensed signal is available, the initial signal $\mathbf{x_{int}}$ can be reconstructed using one of the solvers mentioned in section 1.1. The signal mean is then removed and a 'traditional' systolic peak detector, such as the one described in Lázaro *et al* (2014), is applied on the recovered PPG signal. As an alternative, R peaks from a simultaneously recorded ECG or PPG onsets can be used to define the segments of PPG to be used to generate the template.

Since different onsets can be used, the algorithm is designed to segment the initial PPG based on the type of onset. In particular, when the initial fiducial points are systolic peaks, the PPG is segmented by taking a window of 350 ms before and 500 ms after each detected peak. When ECG R-peaks are used, the PPG window is taken from 50 ms to 900 ms after the fiducial point (R-peak).

To correctly align the segments, the maximum value within each window is used as an anchor point. In such a way the template generation is independent from the reference fiducial point initially used.

At this stage the PPG template γ is computed by taking the mean of the segmented and aligned PPG segments and keeping the window from the minimum (i.e. the onset computed as the max of the third derivative of the template), to 150 ms after the peak. This design optimizes the performance of the detector since keeping only the rising part of γ allows to adapt also to changing rhythm as the pulse width changes with the heart rate. Typically, the PPG shows narrow pulses at high heart rate while, at low heart rate, the pulses are wider.

2.2. Systolic peak detection from estimated correlation

Given a compressed vector $\mathbf{y}$ of length M (corresponding to an uncompressed signal window of length N), the first step is to estimate the correlation $\mathbf{R}_{\mathbf{x}\gamma}$ between $\mathbf{x}$ and the template, from the compressed measurements $\mathbf{y}$ and the (compressed) template γ. In particular, similarly to Da Poian *et al* (2017), we employ the orthogonal estimator, which allows to derive the estimated correlation $\hat{\mathbf{R}}_{\mathbf{x}\gamma,n}$ as

$$\hat{\mathbf{R}}_{\mathbf{x}\gamma,n} = \frac{N}{M}\langle \mathbf{y}, (\Phi\Phi^T)^{-1}\Phi\gamma_n \rangle, \tag{3}$$

where γ_n is the n-sample translated version of the template, whose non-zero elements correspond to the PPG template. (Note that the template is zero-padded to match the uncompressed window length N.)

Prior to peak detection, an exclusion criteria is applied in order to prevent false detections on noisy segments of the PPG signals. The exclusion criterion is based on the correlation energy in the current window $E_{\hat{\mathbf{R}}_{\mathbf{x}\gamma}^{(i)}}$, and the average energy of past windows $\overline{E}_{\hat{\mathbf{R}}_{\mathbf{x}\gamma}}$ (which is updated after a window is considered valid and used for peak detection). In particular, peak detection is not performed on the current window if the ratio $E_{\hat{\mathbf{R}}_{\mathbf{x}\gamma}^{(i)}} \backslash \overline{E}_{\hat{\mathbf{R}}_{\mathbf{x}\gamma}}$ is lower than th_{energy} or higher than th_{energy}^{-1}. Indeed, sudden changes in the correlation value can be associated, with high probability, with noise in the signal and will lead to false detections.

The second stage of the detection procedure consists in the detection of the systolic peaks p by comparing the value of the correlation against an adaptive amplitude-dependent threshold th. The detection threshold is computed for each correlation window, i.e. for each measurement block, and it depends on the correlation amplitude

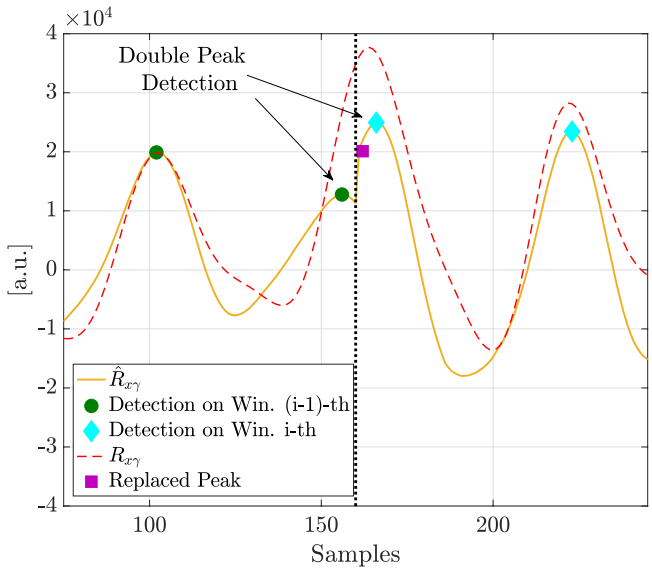

Figure 1. Example of double peak detection on the estimated correlation $\hat{R}_{x\gamma}$ (solid line) due to the transition between two windows. The 'original' correlation $R_{x\gamma}$ is reported for reference (dash line). Signal sampling frequency 125 Hz.

in the current window, $th = th_{corr} \cdot \max(\hat{\mathbf{R}}_{\mathbf{x}\gamma,n})$. A refractory period of 200 ms is used accordingly to physiological limits to prevent double peaks detection.

Additional control to avoid double detection between two consecutive windows, as well as missing detection, is performed. In particular, if the distance (d_{peaks}) between the last peak p_- in the previous window and the first in the current one p_+ is lower than a limit F_{min} the two detections are merged by taking a weighted point in between depending on the values of correlation of both points, i.e. $p_{merged} = (p_- \cdot \hat{\mathbf{R}}_{\mathbf{x}_-\gamma,\mathbf{p}_-} + p_+ \cdot \hat{\mathbf{R}}_{\mathbf{x}\gamma,\mathbf{p}_+})/(\hat{\mathbf{R}}_{\mathbf{x}_-\gamma,\mathbf{p}_-} + \hat{\mathbf{R}}_{\mathbf{x}\gamma,\mathbf{p}_+})$, where $\hat{\mathbf{R}}_{\mathbf{x}_-\gamma,\mathbf{p}_-}$ is the value of the estimated correlation on the previous windows in p_- and $\hat{\mathbf{R}}_{\mathbf{x}\gamma,\mathbf{p}_+}$ for the current in p_+. The example illustrated in figure 1 helps to understand the double peaks replacement.

Whereas, when d_{peaks} is higher than the upper physiological limit F_{max}, a missing peak is highly probable and a second peak search is therefore performed on the estimated correlation between the two windows (in a neighborhood centered on the edge and with length $T_{border}Fs$ samples, Fs being the sampling frequency) by lowering the previous threshold, i.e. $th = th_{border} \cdot th$. The same strategy is also applied if d_{peaks} is higher than th_{IBI} the median IBI (e.g. variation of more than 60% of the median IBI) interval computed on the last N_{IBI} windows.

The actual parameter values used in the experiments will be specified in section 4.1.

2.3. Photoplethysmogram sparsifying dictionary

Despite the proposed method works in the compressed domain without requiring signal reconstruction, it is always possible to recover the original signal from the compressed measurements in order to perform an offline automated analysis or visual evaluation of the signal. To this end, it is necessary to employ a good sparsifying basis or dictionary able to ensure signal reconstruction even at a high compression ratio. In this work we suggest to use the overcomplete dictionary (*PPG Dic.*) described in this section.

In order to design a good mathematical model, we looked at features inside the PPG waveform such as the systolic peak of PPG, always present if the signal is well detected by the device (see figure 2). Another important feature is the slope of the derivative for the first rising portion of PPG. Indeed, the derivative is always positive till it reaches zero at the maximum and changes sign. A last feature is the presence, not in all cases, of a second maximum (diastolic peak) with a lower peak value compared to the previous one. This signal segment can be well approximated by the same basis but scaled and shifted. The aim is to find a family of functions in the form

$$f(a,b,t) = \phi\left(\frac{t-b}{a}\right), \tag{4}$$

whose superposition will approximate the PPG signal, where a, b are parameters respectively for scale and translation.

A good candidate to approximate the one-peak PPG waveform is the following:

$$\phi(t) = t^n \cdot e^{-t}, \tag{5}$$

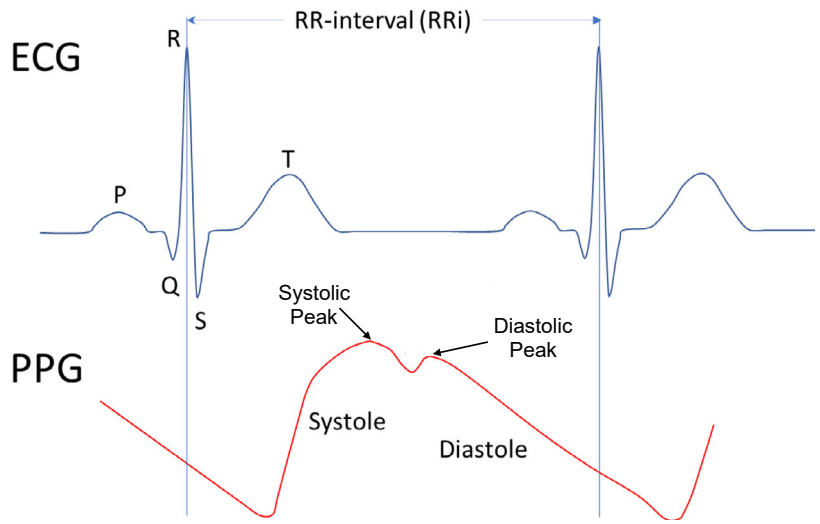

Figure 2. An example of photoplethysmogram (PPG) waveform signal and its characteristic parameters.

for $t \geqslant 0$. Furthermore, such basis functions have another degree of freedom which is the parameter n, whose higher values correspond to steeper rising.

For all the reasons explained above, we propose

$$f(a, b, n, t) = \left(\frac{t-b}{a}\right)^{n} \cdot e^{-\left(\frac{t-b}{a}\right)} \tag{6}$$

for $t > b$ (and 0 elsewhere), as the family of functions used to generate the dictionary.

A value of n which well approximates the rising section of the signal is $n = 2$, and for it the set of suitable a_i found through fitting is $\{a_i | a_i = 1 + 0.5 \cdot k, 0 \leqslant k \leqslant 9\} \cdot \frac{Fs}{60}$ where Fs is the signal sampling frequency.

Figure 3 shows how different numbers of dictionary atoms can approximate a PPG (using the OMP reconstruction algorithm).

3. Materials

3.1. Benchmark datasets

To validate the proposed method we used three different public datasets of PPG signals both from wrist devices and finger tip devices (see table 1). In particular, the first dataset section 3.1.1 was used as a baseline for detection when no physical activity is performed. The second dataset section 3.1.2 was used to test the ability of dealing with rapid changes in heart rate and noise due to physical activity. Finally, the third dataset section 3.1.3 provided a validation for the ability of the proposed method to work with signals containing different kinds of arrhythmias.

3.1.1. IEEE respiratory rate benchmark (RRB) dataset

The pulse oximetry benchmark dataset, was originally proposed for the validation of the SmartFusion respiratory rate estimation algorithm (Karlen *et al* 2013).

The used test set includes 8 min long raw PPG signals (with additional synchronized ECG signals) from 42 subjects, as well as pulse peak and artefact labels validated by an expert rater. All signals were sampled at 300 Hz and recorded from patients with age range 0.8–75.6 years.

3.1.2. IEEE Signal Processing Cup (SPC) dataset

The second dataset used in this work was set up for the IEEE Signal Processing Cup and is publicly available (Zhang 2015). The dataset consists of 12 5 min recordings which were collected from 18 to 58 year old subjects performing various physical exercises. For each subject, the PPG signals were recorded from the wrist using two pulse oximeters with green LEDs (wavelength: 515 nm). The ECG signal was recorded simultaneously from the chest using wet ECG sensors. All signals were sampled at 125 Hz. Three types of activities were performed including walking or running on a treadmill at different speeds from 1–2 km h^{-1} to a maximum of 12–15 km h^{-1}. The subjects were asked to purposely use the hand with the wristband to pull clothes, wipe sweat on forehead,

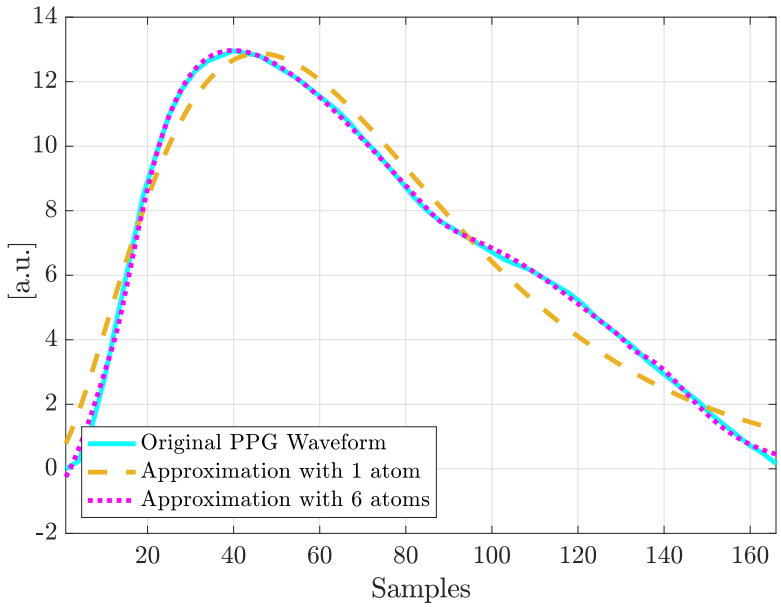

Figure 3. Signal approximation of a PPG pulse (sampled at 300 Hz) using the proposed PPG over-complete dictionary and the OMP method for different sparsity levels 1 and 6. It can be seen that 6 atoms allow a good approximation of the original signal preserving the PPG peak position.

Table 1. Summary of datasets used by this work.

Dataset	Number of signals	Total length (h)	Arrhythmias
Respiratory rate benchmark (RRB) (Karlen *et al* 2013)	42	5.6	No
2015 Signal Processing Cup (SPC) (Zhang 2015)	12	1	No
PhysioNet Challenge 2015 (PC2015) (Clifford *et al* 2015)	550	45.8	yes

and push buttons on the treadmill. The ECG-based HR ground-truth using an 8 s sliding window (2 s increment) is also provided.

3.1.3. PhysioNet Challenge 2015 (PC2015) dataset

The last dataset used in this work is the one provided for the PhysioNet Challenge 2015 (Goldberger *et al* 2000, Clifford *et al* 2015). Data are sourced from four hospitals in the USA and Europe, chosen at random. The dataset contains 750 recordings from which we used a subset of 550 signals excluding those with missing ECG and/or PPG signals or containing very noisy ECG signals that makes it impossible to get a reliable reference. The subset contains synchronized 300 or 330 s long ECG and PPG signals, which have been resampled (using anti-alias filters) to 12 bit, 250 Hz. The signals were preprocessed with a band pass filter at 0.05 to 40 Hz, and mains notch filters applied to remove noise. The following 5 types of arrhythmias are present in the chosen subset: asystole (64 signals), extreme bradycardia (67 signals), extreme tachycardia (99 signals), ventricular tachycardia (290 signals) and ventricular flutter/fibrillation (30 signals).

4. Methods

4.1. Parameter selection

The parameters applied for the validation of the proposed *CSMFppg* are the same for all the datasets, and are listed in table 2. The only parameters that depend on the dataset, and in particular on the sampling frequency, are the ones multiplied by *Fs*.

The choice of *Fmin* and *Fmax* is based on a physiologically probable range of HR ranging between 33 and 200 beats per minute (bpm) for a population likely to use wearable sensors. Note that these parameters are used as a flag to check for missing/double peaks. However, the algorithm is still able to detect peaks such that the inter-beat-interval is shorter or longer then *Fmin* and *Fmax*.

Remark. Optimized settings for the proposed method were obtained by using as training set PPG signals from the MIMIC II dataset (Goldberger *et al* 2000, Saeed *et al* 2011). No further optimization was carried out on the benchmark datasets, which have been used only as 'test' datasets.

Table 2. List of *CSMFppg* parameters and values used by this work.

Parameter	Value	Usage
th_{energy}	5 (%)	Exclusion threshold
F_{min}	0.3 (s)	Minimum inter-beat-interval
F_{max}	1.8 (s)	Maximum inter-beat-interval
$MinVal$	0 (a.u.)	Minimum height of $\mathbf{R}_{\mathbf{x}\gamma,n}$ for detection
th_{corr}	30 (%)	Threshold for detection of peaks referred to maximum peak
T_{border}	0.05 (s)	If one peak is missing, look inside a window of width $T_{border}Fs$ samples centered between two consecutive windows
th_{border}	50 (%)	If in this neighborhood there is a peak higher than Th_b times the weighted mean of two adjacent, detect it
N_{IBI}	10	Compute median IBI on last N_{IBI} windows
th_{IBI}	60 (%)	Maximum % variation of IBI with respect to the median IBI
T_{int}	30 (s)	PPG signal length used to generate the template
L_{win}	1.28 (s)	Length of the PPG window to compress

It should be noted that the results of the proposed method are slightly dependent on the window length N as long as $L_{win} = N/Fs$ ranges between 1 s and 2 s. Shorter windows introduce more artefacts due to discontinuities between consecutive windows. Longer windows, other then increasing the computational load, are not suitable for on-line analysis.

4.2. Validation procedures

To assess the feasibility and actual usefulness of the proposed method, we performed a set of validation experiments on the three datasets described in section 3.1.

In particular we validated and compared the peak detection performance (section 4.2.1), the execution time performance (section 4.2.2) and the reliability of PRV measures estimation (section 4.2.3) on compressed, reconstructed and original signals as follows.

All the signals from the three datasets described in section 3.1 were compressed at several compression ratios, i.e. CR = (5, 10, 20, 30, 40, 50, 60, 65, 70, 75, 80, 82.5, 85, 87.5, 90, 92.5, 95, 97.5)%, by using a random Gaussian sensing matrix. We chose to use a different sensing matrix for each signal to consider its influence on the average detection capability (however, this is not necessary in an actual implementation). After compression all the following methods were applied to the compressed signals and results compared.

- The proposed compressed peak detector *CSMFppg* was applied directly on each compressed signal $\mathbf{y}$, using parameters described in section 4.1.
- Each compressed signal was also reconstructed by using the Sl0 algorithm (Mohimani *et al* 2009) in combination with the proposed PPG Dictionary (*Sl0&PPG Dictionary*). On the obtained reconstructed signal the PPG peak detector proposed by Lázaro *et al* (2014) was applied. It should be noted that it works offline on the entire reconstructed signal (*Offline PD*). Note that the detector in Lázaro *et al* (2014) consists of two phases: a linear filtering transformation (linear-phase FIR low-pass-differentiator filter with transition band from 7.7 Hz to 8 Hz), and an adaptive thresholding operation.
- A second method for reconstructed signals was applied, again we used the Sl0 algorithm but this time in combination with a sparsyfing Wavelet DB4 basis with 3 levels of decomposition (*Sl0&DB4*) (Pinheiro *et al* 2010). The PPG peak detector (*Offline PD*) described above was used to perform offline PPG fiducial point detection.

We also applied the offline systolic peak detector (*Offline PD*) to the entire uncompressed and filtered signal to derive baseline performances.

Finally, for the HRV assessment we also included in the comparison an offline onset detector (*Offline OD*), allowing for further comparison. After subtracting the signal mean, the signal were bandpass filtered to remove frequencies outside the range of 0.2–10 Hz, using a butterworth filter of order three. On the filtered signals we applied the onset detector provided in Vest *et al* (2018), which is a Matlab implementation of the atrial blood pressure onset detector proposed in Zong *et al* (2003).

4.2.1. Detection performance

By evaluating the ability of correct detection of peak locations and comparing it with a standard off-line peak detector, we aim at quantifying the performance of the proposed method, at different compression ratios, taking the ground truth as reference.

Peaks obtained from the four different approaches described in section 4.2 were tested according to the recommendation of the American National Standard for ambulatory ECG analyzers (ANSI/AAMI EC38-1994) (AAMI 1994). For each recording, we computed the sensitivity (Se), the positive predictive value (PPV) and the F1 measure, defined as the harmonic mean of Se and PPV, namely

$$\mathrm{Se} = \frac{\mathrm{TP}}{\mathrm{TP} + \mathrm{FN}} \times 100,$$

$$\mathrm{PPV} = \frac{\mathrm{TP}}{\mathrm{TP} + \mathrm{FP}} \times 100,$$

$$\mathrm{F1} = \frac{2\mathrm{TP}}{2\mathrm{TP} + \mathrm{FN} + \mathrm{FP}} \times 100.$$

In the above equations, TP (true positives) is the total number of systolic peaks correctly located by the detector, a false negative (FN) occurs when the algorithm fails to detect a true peak and a false positive (FP) represents a false beat detection. The average results in terms of Se, PPV and F1 over all the segments are reported.

As reference annotations we used the true PPG peaks provided with the dataset when available. This was the case of the RRB dataset.

For the other two datasets, i.e. SPC and PC2015, we used the QRS-synchronized beat annotations obtained from the ECG signal using *jqrs* (Behar *et al* 2014). Each detected R-peak was associated with the location of the PPG peak. PPG reference beats and detected PPG peaks are matched if the latter fall within a 150 ms window centered at the ECG beat annotation label, as also used for R-peak detection algorithm validation (AAMI 1994).

4.2.2. *Runtime performance*

The usefulness of a compressed peak detector for low-power devices is also related to its capability to be less complex than standard methods working on uncompressed or reconstructed signals. To this end, the complexity of our algorithm has been compared against the offline peak detector proposed in Lázaro *et al* (2014) on uncompressed data and also with respect to the time required for signal reconstruction and peak detection. In particular we are here interested in the performance gain achieved by not recovering the signal. Thus, we evaluated the time required by the proposed method *CSMFppg* and by *Offline PD* as well as by *Sl0&PPG Dic. + Offline PD* and *Sl0&DB4 + Offline PD* (see section 4.2.1). All the simulations were written in Matlab, running on an Intel Core i5 processor, equipped with 8 GB memory.

4.2.3. *Heart rate variability performance*

The last assessment aims to evaluate the impact of compression on the estimated PRV metrics. Differently from peak detection performance, evaluating the ability of the proposed method to derive metrics used in clinical applications allowed to have a better understanding of its possible practical and clinical usability. In this work, we focus on three widely used time domain metrics: the mean of Normal-to-Normal (NN) intervals *NNmean*, the standard deviation of NN *SDNN*, and the root-mean-squared value of the difference (RMSSD) were computed on 60 s epochs with a 10 s increment, using the PhysioNet cardiovascular signal toolbox with default settings (Vest *et al* 2018)[4]. As mentioned, R-peak locations were available for the RRB dataset and derived directly from the ECG signals using *jqrs* (Vest *et al* 2018) for the other datasets. IBIs from uncompressed PPGs where derived using the peaks detected using the *Offline PD* (Lázaro *et al* 2014) and from onsets detected by the *Offline OD* (Vest *et al* 2018). For the compressed scenario, we limited the analysis to IBIs derived from peaks detected directly in the compressed domain with *CSMFppg*. The agreement between the HRV and PRV metrics were assessed using the Bland–Altman method (Bland and Altman 1986). Results are reported as the mean (μ) and the standard deviation (σ) of the difference. One should keep in mind that minor differences between the HRV and PRV exist (Schäfer and Vagedes 2013) and will be an additional source of error in the reported results. We would like to clarify also that the aim of this analysis is to show that errors deriving from using the proposed *CSMFppg* are comparable with those obtained on the uncompressed PPG signal with a standard detector. It is beyond the scope of this paper to prove whether or not HRV metrics derived from PPG could be used as a surrogate measurement of HRV from the ECG.

5. Results

5.1. Detection performance

Table 3 reports the F1 measure obtained using the proposed method for different compression ratios and separately for each dataset in order to understand the performance and limitations based on the type of signals. Additional results for Se, PPV and F1 measure are reported in table A1

[4] Open source code available on-line https://doi.org/10.5281/zenodo.1243111, accessed on 06 September 2018.

Table 3. Detection performance of the PPG systolic peak detection performed on compressed sensed data using the proposed *CSMFppg* at different compression ratios. The results for F1 measure (F1) are reported as mean ± std for each of the three datasets used as well as for the training data.

	0%	10%	20%	30%	40%	50%	60%	70%	80%	90%
Training	95.57 ± 5.0	93.5 ± 5.5	93.2 ± 5.8	93.3 ± 5.7	93.5 ± 5.5	92.9 ± 5.9	91.8 ± 6.9	89.6 ± 8.4	84.2 ± 9.0	76.4 ± 11.4
RBB	99.2 ± 3.3	99.1 ± 1.3	99.1 ± 1.3	99.0 ± 1.3	98.9 ± 1.4	98.9 ± 1.7	98.9 ± 1.5	98.7 ± 1.7	98.4 ± 2.2	95.9 ± 5.1
SPC	89.1 ± 4.9	90.3 ± 5.0	90.5 ± 4.5	89.5 ± 5.2	90.0 ± 5.1	88.7 ± 5.4	88.2 ± 5.3	87.2 ± 7.0	84.4 ± 5.0	77.6 ± 7.4
PC2015	90.6 ± 11.4	90.2 ± 8.4	89.9 ± 8.7	89.7 ± 9.0	89.6 ± 9.1	89.2 ± 9.2	88.9 ± 9.4	88.1 ± 9.8	86.5 ± 10.3	81.4 ± 11.6

Notes: The 0% compression reports the results of the offline peak detector (Lázaro *et al* 2014) on the original uncompressed data as a reference.

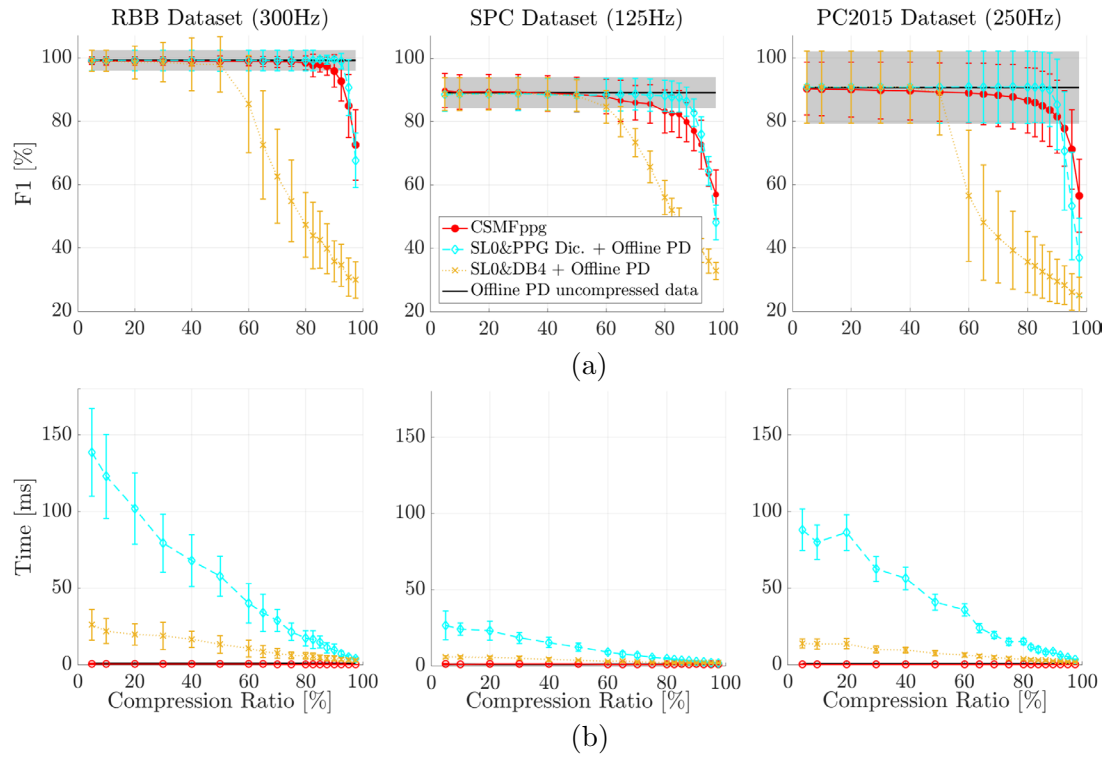

Figure 4. (a) Performance of different PPG detection approaches on compressed sensed data and (b) required execution time. For each dataset considered in this work the F1 value (mean ± standard deviation) is reported in a separated plot. The time required to process 1 s of signal is reported as (mean ± standard deviation). Each plot reports the results for the proposed method working directly on the compressed measurements (*CSMFppg*), after signal reconstruction using *Sl0&PPG Dic.* or *Sl0&DB4* applying an offline peak detector (*Offline PD*). Also results for offline peak detection (*Offline PD*) on the uncompressed data are reported as a reference (black solid line, bars represent the standard deviation).

Detection on uncompressed signals is marked as 0% compression and, especially for the dataset where no PPG peaks were given as reference, provides an upper bound for the detection performance.

Figure 4(a) provides a comparison of the *CSMFppg* method and the detection after signal reconstruction with different bases in terms of average F1 measure. Figure 4(a) also reports the results for uncompressed data.

Figure 5(a) shows an example of peak detection on record 08_TYPE02 performed by CSMFppg at CR = 75% (red crosses) and also by using the peak detector in Lázaro *et al* (2014) (black circles). Reference peaks are marked by yellow diamonds.

5.2. Runtime performance

The computational load for the different methods is reported in figure 4(b). We report the execution time for one window corresponding to 1 s. The results are shown separately for each dataset to highlight the impact of different sampling frequencies, in particular on methods that require signal reconstruction before peak detection. For all the dataset the proposed *CSMFppg* is up to ∼100 time faster than reconstruction using the PPG Dictionary.

To process 1 s of a signal, the offline peak detector (Lázaro *et al* 2014) requires an average time of 0.5 ± 0.2 ms. Whereas, the proposed *CSMFppg*, which allows data compression, requires at most 0.3 ± 0.2 ms. Finally, the two methods based on signal reconstruction prior to peak detection, i.e. the *Sl0&PPG Dic.* and the *Sl0&DB4*, require up to 90 ± 22 ms and 15 ± 5 ms, respectively.

5.3. Heart rate variability performance

Table 4 reports the accuracy of PRV metrics, with respect to HRV metrics computed from ECG, as mean and standard deviation of the difference. The impact due to compression is negligible and the error is similar to that obtained when computing HRV metrics on ECG and on uncompressed PPG signals, at least for compression ratios lower than 80%. Due to the limited space, only one example of the Bland–Altman analysis is shown in figure 6 for the SDDN parameter calculated on the RBB dataset. Taking the SDNN metric calculated from the synced ECG as reference, figure 6(a) shows the mean and the difference between the reference and the same metric calculated from the PPG signals with the Offline PD on uncompressed data. Each mark in the figure represents the mean and the difference

Table 4. Pulse rate variability measurement accuracy using Bland–Altman (Bland and Altman 1986) analysis, mean (μ) and standard deviation (σ) of the difference are reported. HRV metrics derived from simultaneous ECG signals are used as reference.

	RRB						SPC						PC2015					
	NNmean (ms)		SDNN (ms)		RMSSD (ms)		NNmean(ms)		SDNN (ms)		RMSSD (ms)		NNmean (ms)		SDNN (ms)		RMSSD (ms)	
	μ	σ	μ	σ	μ	σ	μ	σ	μ	σ	μ	σ	μ	σ	μ	σ	μ	σ
PRV computed on uncompressed and filtered PPG signals																		
Detector																		
Lázaro *et al* (2014)	0	10	−6	11	−12	11	−28	55	−45	48	−52	45	1	45	−16	39	−23	43
Vest *et al* (2018)	11	68	−10	15	−20	26	−34	80	−56	56	−58	43	8	49	−17	35	−26	40
PRV computed on compressed PPG signals using *CSMFppg*																		
CR (%)																		
5	0	3	−6	8	−14	12	−42	76	−59	50	−68	50	−7	34	−21	45	−31	49
10	0	3	−7	8	−15	13	−41	77	−56	50	−65	51	−6	31	−22	46	−32	50
20	0	3	−8	9	−17	14	−42	77	−56	52	−64	53	−8	46	−26	53	−37	57
30	0	2	−8	6	−17	11	−44	77	−57	49	−70	52	−9	46	−27	55	−38	58
40	0	4	−9	12	−19	15	−39	76	−56	48	−64	47	−10	66	−31	57	−42	63
50	0	2	−9	7	−20	11	−42	75	−55	49	−64	47	−7	57	−33	58	−46	63
60	0	3	−11	9	−23	14	−34	65	−58	43	−67	44	−4	63	−33	52	−47	57
65	0	3	−12	12	−26	16	−47	77	−61	43	−78	47	−7	96	−36	61	−51	66
70	0	3	−13	7	−27	10	−39	78	−53	46	−63	43	−11	111	−41	62	−57	70
75	0	4	−15	14	−32	19	−45	77	−62	45	−75	43	−16	113	−47	71	−67	83
80	1	7	−19	18	−38	22	−35	62	−57	41	−71	42	−10	125	−51	68	−70	74
82.5	0	5	−18	14	−37	19	−67	81	−74	45	−88	43	−11	124	−55	72	−76	79
85	0	6	−22	16	−44	22	−66	89	−68	41	−84	39	−19	156	−65	77	−87	85
87.5	−1	8	−25	21	−48	25	−51	81	−64	43	−82	44	−14	163	−70	84	−94	100
90	1	6	−28	13	−56	20	−49	69	−67	48	−82	48	−6	165	−74	78	−99	87
92.5	2	15	−37	25	−67	31	−67	73	−74	34	−97	35	−10	202	−81	77	−103	78
95	27	66	−66	52	−94	50	−64	71	−76	44	−103	47	6	239	−89	77	−113	86
97.5	61	90	−93	48	−123	52	−52	99	−66	55	−94	56	29	268	−86	76	−107	81

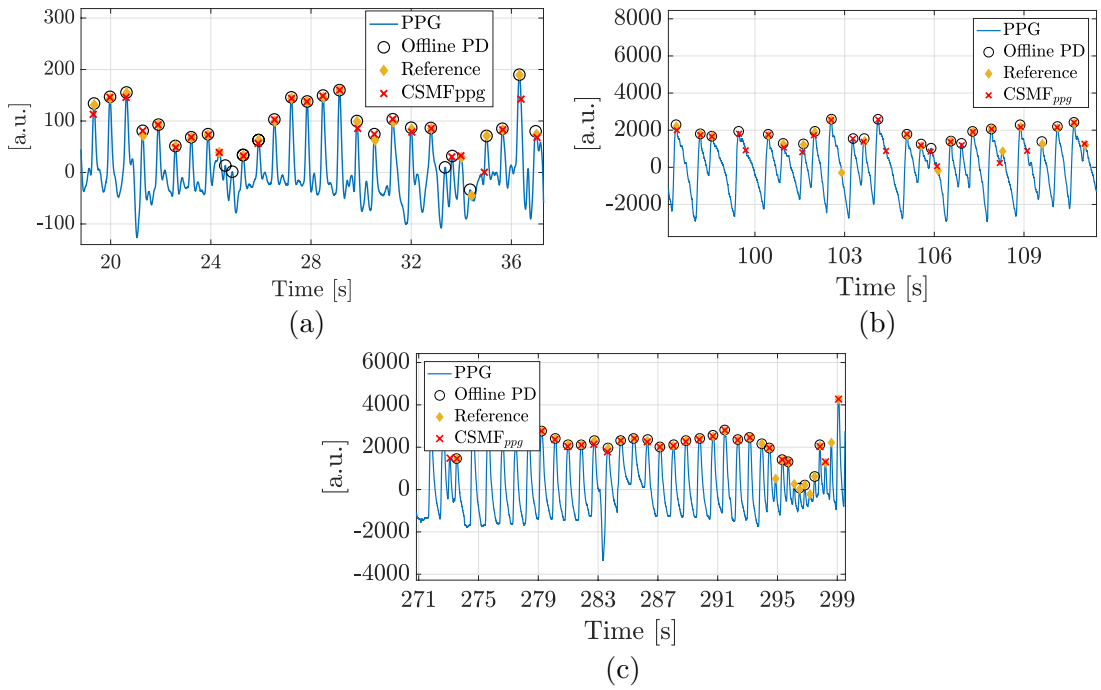

Figure 5. Example of peaks detected with the proposed CSMFppg on compressed PPG ((a) CR = 75%, ((b) and (c)) CR = 60%), red crosses, and on original PPG with (Lázaro *et al* 2014), black circles. (a) Signal 08_TYPE02 from the SPC database, ((b) and (c)) signal f543l and t478s containing ventricular flutter/fibrillation and ventricular tachycardia, respectively—from the PC2015 database. Reference annotations are marked with yellow diamonds.

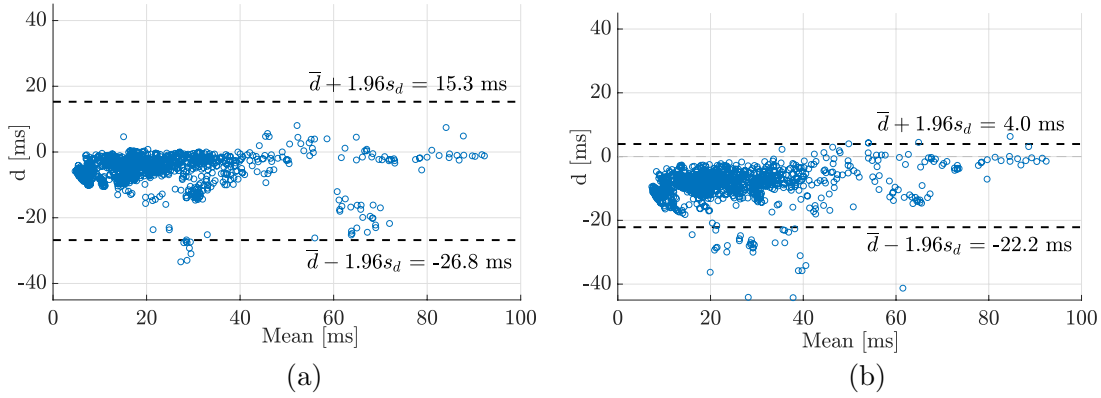

Figure 6. Bland–Altman plot comparing the SDNN from the ECGs with the one from PPGs on the RRB dataset. PRV-SDNN metrics are computed from IBIs detected (a) on the uncompressed PPG signals using the *Offline PD* and (b) directly on the compressd PPG signals (CR = 50%) by using the proposed *CSMFppg*. All metrics are computed on 60 s windows with 10 s increment.

of the metrics computed on a 60 s window with 10 s increment. Figure 6(b) shows the mean and the difference of the reference with the proposed *CSMFppg* at 50% compression. The 95% limits of agreement are −26.8 ms and 15.3 ms for the PRV computed on the uncompressed data and −22.2 ms and 4 ms for the proposed scheme.

6. Discussion

Detection performance on the three datasets suggests that the proposed method can accurately perform systolic peak detection on compressed sensed data up to CR of 80% without a significant performance loss in terms of pooled F1 measure (87.3% ± 9.7%) with respect to the offline peak detector on the original data (pooled F1 = 90.5% ± 10.7%).

In particular, for the RRB dataset, where true annotations for the PPG peaks were available, the F1 measure for a compression ratio 87.5% (F1 = 97.3% ± 2.9%) is comparable to the one obtained on the original uncompressed signal by an offline peak detector (F1 = 99.2% ± 3.3%). For the SPC dataset, the F1 measure (F1 = 89.1% ± 4.9%), starts to drop for the proposed *CSMFppg* at compression ratios higher than 60%. On the

last dataset, PC2015, which included also different types of arrhythmias, we have a 2% drop on the F1 measure for the proposed method at CR = 65% (reference offline F1 measure equal to 90.6% ± 11.4%).

With respect to the sensitivity and positive predictivity, we notice that the proposed method has typically a higher PPV than Se, which is somehow preferable when the future step is HRV analysis. Indeed, wrong detection due to noise might lead to misclassification of arrhythmias. The PC2015 dataset was used to test performance on recordings containing abnormal rhythms. Based on the description provided with the dataset[5], an alarm was triggered 5 min from the beginning of each record and the onset of the event is within 10 s of the alarm, although additional arrhythmia events can be present in the 5 min preceding the alarm. Unfortunately, it is impossible to establish the exact prevalence of the irregular rhythms without specific annotations or to provide specific performance for the abnormal segments of the recordings. By visual inspecting some of the recordings, we noticed that one possible limitation of the proposed method is the detection of peaks during ventricular tachycardia episodes, when some of the PPG peaks have a very low amplitude (see figure 5(b)). With other types of arrhythmia, such as ventricular tachycardia/fibrillation, the proposed method is able to perform as well as the offline peak detector (see figure 5(c)). Overall, our results on both onset detection performance and HRV metrics are comparable with those obtained by offline methods suggesting that the use of the *CSMFppg* is not limited to a healthy population but can be also applied for clinical purposes.

As expected, detection after signal reconstruction is highly dependent on the sparsifying basis/dictionary adopted. It can be seen from the F1 measure reported in figure 4(a) that the dictionary proposed in this work performs slightly better than the other methods (i.e. detection using *CSMFppg* or detection after *Sl0&DB4*). However, this comes at the cost of high computational complexity, as shown in figure 4(b).

A first analysis of PRV metrics extracted from compressed signals allow us to conclude that the proposed method provide results consistent with those derived from the original PPGs.

Future work will analyze the use of IBIs extracted with the proposed method combined with low-complexity signal classification algorithms for arrhythmia detection.

Giving similar detection performance, the proposed method is competitive in terms of computational cost with respect to peak detection after signal reconstruction. However, further studies are required to evaluate the actual energy saving or battery life extension for a given compression ratio. Indeed, the compression ratio required to achieve a certain battery extension is not only dependent on the device and hardware configuration, but also on the CS approach adopted (analog versus digital). Based on our preliminary study in Da Poian *et al* (2016), a CR⩾50% would allow for a significant energy saving when digital CS is used, extending the battery life of at least a factor two.

The next challenge is the implementation of an actual system with good enough performance at the lowest possible power consumption. Moreover, an auto-adaptive algorithm that increases the compression ratio when possible can help to improve the overall performance and to find the best trade-off for accuracy and power consumption.

7. Conclusions

A wearable health monitoring device should be capable of measuring multiple parameters with accurate readings and having a long battery lifetime. In this work, we presented a PPG systolic peak detector able to work directly on the compressed sensed signals. The method is particularly suitable for low-power implementation on wearable devices or smartphones. While the simultaneous acquisition and compression of the signal by means of analog compressive sensing reduces the sensing energy, the proposed method allows for low-power on-line signal analysis. The pooled average F1 measure for the proposed *CSMFppg* method ranges from 91% at CR = 5% to 82% at CR = 90%, and is consistent with offline methods on uncompressed and filtered signals (F1 = 91%). The main advantage is the possibility to perform PPG analysis directly on the wearable device or on a smart-phone in a real-time application. Therefore, whether the data are processed on the device or sent to the smart-phone, compressive sensing combined with the proposed method will help to extend the battery life.

Acknowledgments

The authors wish to acknowledge the National Institutes of Health Grant # R01 HL136205 and the National Science Foundation Award 1636933. Any opinions, findings, and conclusions or recommendations expressed in this material are those of the author(s) and do not necessarily reflect the views of the National Science Foundation or the National Institutes of Health.

Appendix

In this appendix, we report some additional results about the performance of the proposed PPG systolic peak detector. The results are reported in table A1.

[5] https://physionet.org/physiobank/database/challenge/2015/

Table A1. Performance of the PPG systolic peak detection performed on compressed sensed data using the proposed *CSMFppg* at different compression ratios. The results for Sensitivity (Se), positive predictivity (PPV) and F1 measure (F1), are reported as mean ± std for each of the three dataset used.

	RRB			SPC			PC2015		
CR (%)	Se (%)	PPV (%)	F1 (%)	Se (%)	PPV (%)	F1(%)	Se (%)	PPV (%)	F1 (%)
0	99.6 ± 0.3	99.1 ± 5.4	99.2 ± 3.3	90.5 ± 3.6	88.0 ± 7.0	89.1 ± 4.9	92.4 ± 11.6	89.8 ± 11.6	90.6 ± 11.4
5	98.7 ± 1.8	99.5 ± 1.1	99.1 ± 1.3	86.5 ± 6.5	94.8 ± 3.7	90.4 ± 4.8	90.0 ± 9.6	91.2 ± 8.9	90.3 ± 8.4
10	98.7 ± 1.8	99.4 ± 1.0	99.1 ± 1.3	86.3 ± 6.6	94.8 ± 3.9	90.3 ± 5.0	90.0 ± 9.6	90.9 ± 9.2	90.2 ± 8.5
20	98.7 ± 1.8	99.4 ± 1.1	99.1 ± 1.3	86.7 ± 6.2	94.7 ± 3.9	90.5 ± 4.5	89.9 ± 9.6	90.6 ± 9.4	89.9 ± 8.7
30	98.7 ± 1.8	99.4 ± 1.1	99.0 ± 1.3	85.2 ± 6.9	94.3 ± 3.8	89.5 ± 5.2	89.7 ± 9.8	90.2 ± 9.8	89.7 ± 9.0
40	98.6 ± 2.1	99.3 ± 1.3	98.9 ± 1.4	86.3 ± 6.8	94.2 ± 4.1	90.0 ± 5.1	89.7 ± 9.9	90.0 ± 10.0	89.6 ± 9.1
50	98.5 ± 2.3	99.3 ± 1.4	98.9 ± 1.7	84.5 ± 6.6	93.4 ± 4.9	88.7 ± 5.4	89.5 ± 9.9	89.6 ± 10.2	89.2 ± 9.2
60	98.6 ± 2.0	99.3 ± 1.3	98.9 ± 1.5	84.2 ± 6.5	92.6 ± 4.8	88.2 ± 5.3	89.3 ± 10.0	89.1 ± 10.5	88.9 ± 9.4
65	98.5 ± 2.4	99.3 ± 1.1	98.9 ± 1.6	82.4 ± 7.5	92.1 ± 4.6	86.9 ± 5.8	89.1 ± 10.2	88.7 ± 10.7	88.6 ± 9.7
70	98.5 ± 2.2	99.0 ± 1.7	98.7 ± 1.7	83.2 ± 8.9	91.8 ± 5.2	87.2 ± 7.0	88.7 ± 10.3	88.2 ± 10.9	88.1 ± 9.8
75	98.6 ± 1.9	99.0 ± 1.6	98.8 ± 1.5	80.4 ± 6.5	90.7 ± 4.6	85.1 ± 5.4	88.4 ± 10.6	87.6 ± 11.3	87.7 ± 10.2
80	98.1 ± 2.6	98.7 ± 2.6	98.4 ± 2.2	80.5 ± 5.6	88.8 ± 5.2	84.4 ± 5.0	87.3 ± 10.8	86.4 ± 11.4	86.5 ± 10.3
82.5	97.7 ± 3.3	97.5 ± 4.4	97.6 ± 3.6	75.0 ± 5.2	88.1 ± 5.0	81.0 ± 4.6	86.8 ± 11.1	85.6 ± 12.0	85.9 ± 10.8
85	97.7 ± 3.0	98.2 ± 2.4	97.9 ± 2.4	74.3 ± 6.4	86.8 ± 5.6	80.0 ± 5.5	85.9 ± 11.4	84.4 ± 12.2	84.8 ± 11.1
87.5	97.4 ± 3.0	97.4 ± 3.6	97.3 ± 2.9	73.6 ± 8.8	84.6 ± 5.9	78.6 ± 7.3	84.6 ± 11.8	83.1 ± 12.6	83.5 ± 11.4
90	96.0 ± 4.9	95.8 ± 5.9	95.9 ± 5.1	72.7 ± 7.7	83.4 ± 7.6	77.6 ± 7.4	82.9 ± 11.9	80.7 ± 12.7	81.4 ± 11.6
92.5	93.6 ± 6.0	91.7 ± 7.7	92.5 ± 6.2	66.6 ± 6.5	78.7 ± 4.7	72.0 ± 5.4	79.8 ± 12.0	76.5 ± 13.4	77.7 ± 11.9
95	87.4 ± 7.5	83.0 ± 12.9	84.8 ± 10.0	57.5 ± 7.1	70.2 ± 8.3	63.1 ± 7.5	73.9 ± 12.8	69.3 ± 14.0	71.0 ± 12.6
97.5	77.3 ± 10.4	69.3 ± 13.5	72.6 ± 11.1	52.5 ± 11.3	61.2 ± 11.1	56.3 ± 10.9	60.5 ± 11.5	53.8 ± 13.3	56.4 ± 11.5

Notes: The 0% compression reports the results of the offline peak detector (Lázaro *et al* 2014) on the original uncompressed data as a reference.

ORCID iDs

Giulia Da Poian https://orcid.org/0000-0002-8960-1077

References

AAMI 1994 *American National Standard for Ambulatory Electrocardiographs* (*Publication ANSI, AAMI ec38-1994*) (Arlington, VA: Association for the Advancement of Medical Instrumentation)

Baraniuk R, Davenport M, DeVore R and Wakin M 2008 A simple proof of the restricted isometry property for random matrices *Constructive Approx.* **28** 253–63

Behar J, Johnson A, Clifford G D and Oster J 2014 A comparison of single channel fetal ECG extraction methods *Ann. Biomed. Eng.* **42** 1340–53

Bland J M and Altman D 1986 Statistical methods for assessing agreement between two methods of clinical measurement *Lancet* **327** 307–10

Candès E J and Wakin M B 2008 An introduction to compressive sampling *IEEE Signal Process. Mag.* **25** 21–30

Chen F, Chandrakasan A P and Stojanovic V M 2012 Design and analysis of a hardware-efficient compressed sensing architecture for data compression in wireless sensors *IEEE J. Solid-State Circuits* **47** 744–56

Chen S S, Donoho D L and Saunders M A 2001 Atomic decomposition by basis pursuit *SIAM Rev.* **43** 129–59

Clifford G D, Silva I, Moody B, Li Q, Kella D, Shahin A, Kooistra T, Perry D and Mark R G 2015 The PhysioNet/Computing in Cardiology Challenge 2015: reducing false arrhythmia alarms in the ICU *Computing in Cardiology Conf.* (IEEE) pp 273–6

Craven D, McGinley B, Kilmartin L, Glavin M and Jones E 2015 Compressed sensing for bioelectric signals: a review *IEEE J. Biomed. Health Inform.* **19** 529–40

Da Poian G, Brandalise D, Bernardini R and Rinaldo R 2016 Energy and quality evaluation for compressive sensing of fetal electrocardiogram signals *Sensors* **17** 9

Da Poian G, Rozell C J, Bernardini R, Rinaldo R and Clifford G D 2017 Matched filtering for heart rate estimation on compressive sensing ECG measurements *IEEE Trans. Biomed. Eng.* **65** 1349–58

Dixon A M, Allstot E G, Gangopadhyay D and Allstot D J 2012 Compressed sensing system considerations for ECG and EMG wireless biosensors *IEEE Trans. Biomed. Circuits Syst.* **6** 156–66

Goldberger A L, Amaral L A, Glass L, Hausdorff J M, Ivanov P C, Mark R G, Mietus J E, Moody G B, Peng C K and Stanley H E 2000 Physiobank, PhysioToolkit, and PhysioNet *Circulation* **101** e215–20

Karlen W, Raman S, Ansermino J M and Dumont G A 2013 Multiparameter respiratory rate estimation from the photoplethysmogram *IEEE Trans. Biomed. Eng.* **60** 1946–53

Lázaro J, Gil E, Vergara J M and Laguna P 2014 Pulse rate variability analysis for discrimination of sleep-apnea-related decreases in the amplitude fluctuations of pulse photoplethysmographic signal in children *IEEE J. Biomed. Health Inform.* **18** 240–6

Liu B, Zhang Z, Xu G, Fan H and Fu Q 2014 Energy efficient telemonitoring of physiological signals via compressed sensing: a fast algorithm and power consumption evaluation *Biomed. Signal Process. Control* **11** 80–8

Mohimani H, Babaie-Zadeh M and Jutten C 2009 A fast approach for overcomplete sparse decomposition based on smoothed *l*0 Norm *IEEE Trans. Signal Process.* **57** 289–301

Natarajan V, Dadhich D and Ranganathan K 2017 Compressive sensing sparse sampling photoplethysmogram (PPG) measurement *US Patent* App. 15/089,501

Pamula V R, Van Hoof C and Verhelst M 2018 An ultra-low power, robust photoplethysmographic readout exploiting compressive sampling, artefact reduction, sensor fusion *Hybrid ADCs, Smart Sensors for the IoT and Sub-1V and Advanced Node Analog Circuit Design* (New York: Springer) pp 145–63

Pantelopoulos A and Bourbakis N G 2010 A survey on wearable sensor-based systems for health monitoring and prognosis *IEEE Trans. Syst. Man Cybern.* C **40** 1–12

Pareschi F *et al* 2017 Energy analysis of decoders for rakeness-based compressed sensing of ecg signals *IEEE Trans. Biomed. Circuits Syst.* **11** 1278–89

Pinheiro E C, Postolache O A and Girao P S 2010 Implementation of compressed sensing in telecardiology sensor networks *Int. J. Telemed. Appl.* **2010** 7

Rajesh P V, Valero-Sarmiento J M, Yan L, Bozkurt A, Van Hoof C, Van Helleputte N, Yazicioglu R F and Verhelst M 2016 22.4 A 172 μW compressive sampling photoplethysmographic readout with embedded direct heart-rate and variability extraction from compressively sampled data *IEEE Int. Solid-State Circuits Conf.* (IEEE) pp 386–7

Saeed M, Villarroel M, Reisner A T, Clifford G, Lehman L W, Moody G, Heldt T, Kyaw T H, Moody B and Mark R G 2011 Multiparameter intelligent monitoring in intensive care II (MIMIC-II): a public-access intensive care unit database *Crit. Care Med.* **39** 952

Schäfer A and Vagedes J 2013 How accurate is pulse rate variability as an estimate of heart rate variability?: a review on studies comparing photoplethysmographic technology with an electrocardiogram *Int. J. Cardiol.* **166** 15–29

Seneviratne S, Hu Y, Nguyen T, Lan G, Khalifa S, Thilakarathna K, Hassan M and Seneviratne A 2017 A survey of wearable devices and challenges *IEEE Commun. Surv. Tutorials* **19** 2573–620

Shcherbina A, Mattsson C M, Waggott D, Salisbury H, Christle J W, Hastie T, Wheeler M T and Ashley E A 2017 Accuracy in wrist-worn, sensor-based measurements of heart rate and energy expenditure in a diverse cohort *J. Personalized Med.* **7** 3

Tropp J A and Gilbert A C 2007 Signal recovery from random measurements via orthogonal matching pursuit *IEEE Trans. Inf. Theory* **53** 4655–66

Vest A N, Da Poian G, Li Q, Liu C, Nemati S, Shah A J and Clifford G D 2018 An open source benchmarked toolbox for cardiovascular waveform and interval analysis *Physiol. Meas.* **39** 105004

Zhang Z 2015 Photoplethysmography-based heart rate monitoring in physical activities via joint sparse spectrum reconstruction *IEEE Trans. Biomed. Eng.* **62** 1902–10

Zhang Z, Pi Z and Liu B 2015 TROIKA: a general framework for heart rate monitoring using wrist-type photoplethysmographic signals during intensive physical exercise *IEEE Trans. Biomed. Eng.* **62** 522–31

Zong W, Heldt T, Moody G and Mark R 2003 An open-source algorithm to detect onset of arterial blood pressure pulses *Computers in Cardiology* (IEEE) pp 259–62